SIMULATION OF THE DAMAGE TOLERANCE BEHAVIOUR OF CFRP/HONEYCOMB SANDWICH BASED ON MEASURED PROPERTIES OF THE RESIN IMPREGNATED CORE PAPER

Falk Hähnel and Klaus Wolf

Technische Universität Dresden
Department of Aerospace Engineering
01062 Dresden
Germany
falk.haehnel@tu-dresden.de

ABSTRACT

Honeycomb cores made of phenol resin impregnated paper are widely used in sandwich structures. This paper presents experimental investigations on papers of different phenol resin volume fraction to determine tensile and compressive mechanical properties of the honeycomb cell walls. Simulations of the conducted tests were carried out to calibrate a cell wall material model. Finally, impacts of different energy levels on honeycomb sandwich plates were simulated using a meso-mechanical approach where the honeycomb cell walls are modeled by 2D-shell elements. The obtained simulation results agree very well with the experiments.

1. INTRODUCTION

Structural sandwich is widely used as a lightweight design solution for load-carrying components. In aircraft structures particularly sandwich using carbon fibre reinforced plastics (CFRP) as face sheets and non-metallic honeycombs as core material is applied due to features such as high strength-to-weight and stiffness-to-weight ratios as well as good fatigue behaviour. Owing to the rather weak core material, sandwich is prone to a range of defects and damages as a result of impact loading which may accidentally occur during assembly or operation of aircraft. These damages and their effect on the load carrying capability of the structure have to be considered in the damage tolerant design of aircraft. Therefore, it is necessary to determine the extent of damage in sandwich structures resulting from impact events and to predict the residual strength of the damaged components. Currently, in the development process this task is mainly done experimentally by using drop tests to simulate the impact loading, NDT methods to determine the damage size and compression or shear after impact (CAI, SAI) tests to investigate the residual load carrying capability of the damaged structures. These experimental procedures are rather costly and time consuming. Therefore, much research has been done to develop reliable simulation procedures which are able to predict the damage tolerance behaviour. The simulation tools applied for this task have to be based on close to reality numerical models of the structure which requires a thorough knowledge about the basic material properties of the sandwich constituents.

As long as only the global behaviour of sandwich components is investigated by finite element methods, it is sufficient to model the structure by using shell elements for the skins and solid elements for the core [1, 2]. In the case of honeycomb sandwich such models permit only a macro-mechanical description of the core behaviour. Thus, it is not possible to account for local failure modes of the hexagonal cell structures. Nevertheless, these local effects are important in cases where damage tolerance is of interest. For this kind of problem a detailed modeling of the honeycomb cell structure is required [3-6]. For example, impact loading of honeycomb sandwich results in very

complex damage modes in the core, as can be seen in Figure 1. In the centre of the impact area the honeycomb material is crushed. This damage is mainly the result of local buckling of the cell walls in combination with compressive failure of the core material which is usually a resin-impregnated paper [4-6]. Closer to the edge of the impact area the core is subjected to high shear forces which result in shear cracks in the walls. This clearly shows that material properties such as stiffness and strength of the honeycomb material are crucial parameters for the formation of damage in the sandwich core. Therefore, the knowledge of these properties is essential for a reliable numerical simulation of the damage tolerance behaviour of impact loaded honeycomb sandwich structures.

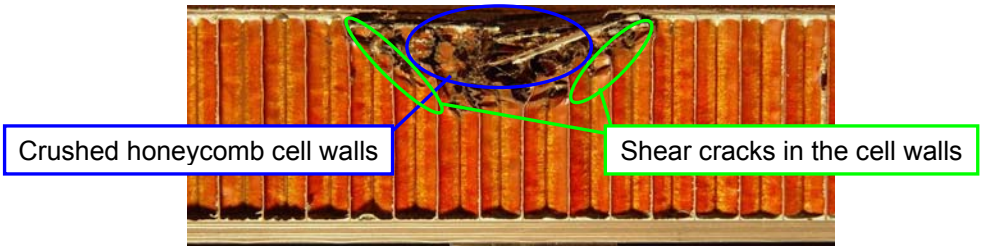

Figure 1: Impact damage of a non-metallic honeycomb sandwich

Usually, honeycomb manufacturers provide material data only for honeycomb blocks instead of the impregnated papers used as core material. Hence, one approach is to determine the paper properties from the global core properties. This can be done by numerical simulation of the tests used to measure the global properties [4]. This approach provides only average data and it is difficult to identify the non-linear behaviour of the material. Thus, in case that a more thorough knowledge is required the material properties of the resin-impregnated paper have to be determined directly by appropriate test procedures [5, 7].

In the research presented in this paper a standard test method for paper and board was used for the identification of tensile properties. Compressive mechanical properties of the different impregnated papers investigated were determined by utilizing a special test method which was improved compared to [4]. These test procedures were used to carry out an extensive test program on different papers which were impregnated with phenol resin. Several parameters such as the paper thickness and the influence of the production process were investigated. Furthermore, numerical simulations of the impact damage process of CFRP-honeycomb sandwich based on the determined core material properties were carried out.

2. EXPERIMENTAL INVESTIGATION

2.1 Materials

During the manufacturing process of honeycomb sandwich cores (Figure 2) the plain paper comes from a coil and goes first through a printer for adhesive lines to be printed. Once the lines are printed, the paper is cut to size and stacked into plies using a stacking machine (1). Next the stacked sheets are pressed using a heated press to allow the adhesive to cure and bond the sheets together (2). The expanded plain paper honeycomb block (3) is dipped into phenol resin (4) and cured (5) to give stability and increase the fire resistance [8]. Depending on the penetrability of the used plain paper the honeycomb cell walls are impregnated or coated with phenol resin as in the case of NOMEX®-honeycombs (Figure 3).

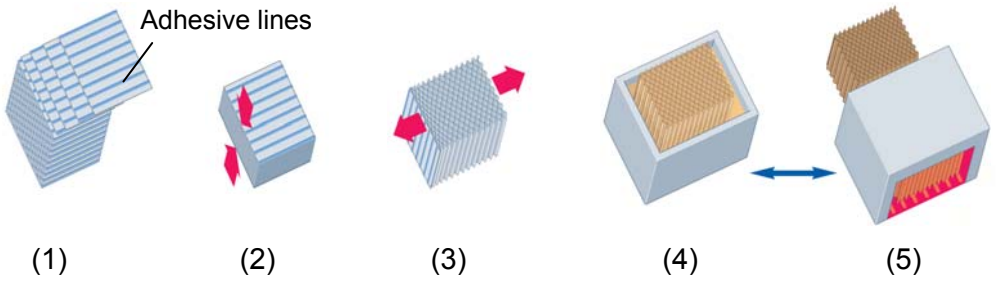

Figure 2: Manufacturing process of phenol resin impregnated honeycomb core [8]

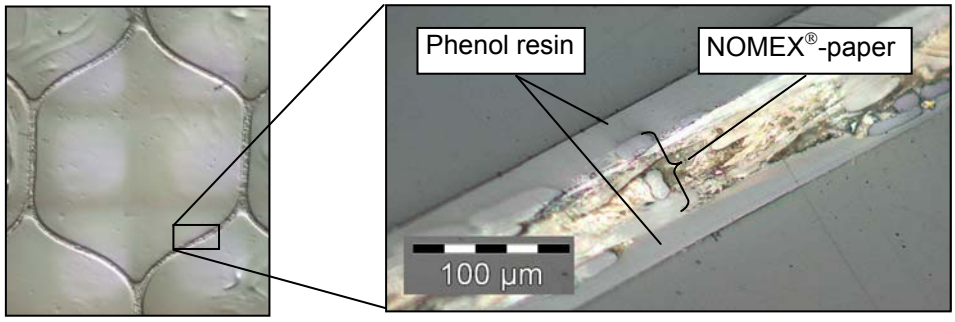

Figure 3: Micrographs of 4.8-64 NOMEX®-honeycomb cell and single cell wall

The basic mechanical properties of the honeycomb materials have to be determined based on specimens which have the same characteristics than the impregnated cell walls. Since the hexagons of the honeycombs usually applied in aircraft structures are rather small, it is not possible to cut the required test specimens directly from the walls. Thus, larger sheets of resin impregnated papers had to be provided by a honeycomb manufacturer. The process applied to these papers was similar to the standard honeycomb production procedure: sheets of plain paper were impregnated once or more times with phenol resin and cured, resulting in resin impregnated paper with different phenol resin volume fraction.

2.1 Tensile test

Test specimens were cut from the available paper sheets along to the machine (0°) and transverse to the machine direction (90°). A *L&W Strip Punch* was used to cut the specimen precisely to 15 mm width according to ISO 1924 and 150 mm length.

The tensile tests were performed using a *L&W Tensile & Fracture Toughness Tester SE 062/064* which is designed to measure and record the tensile strength, strain at break, tensile energy absorption and tensile stiffness of paper. The pneumatic fixtures of the L&W tester clamp the specimens on both sides at a free length of 100 mm. All tested specimens were pulled with a constant rate of 6 mm/min.

Figure 4a shows measured force-elongation functions of specimens with different resin volume fraction which were loaded in machine and transverse direction. A distinct bi-linear elastic-plastic behaviour could be found for the plain paper whereas the impregnated specimen has a nearly complete linear elastic one.

To calculate the engineering stress-strain function as well as material constants such as the Young's modulus the thickness of specimens was determined from micrographs of paper cross sections. The mean thicknesses obtained are 0.087 mm for the plain paper (φ=0.00) and 0.193 mm for the impregnated one (φ=0.55). The calculated stress-strain functions show that the impregnated paper fails close to 1% strain for both load

directions (Figure 4b). The failure of these specimens is caused by the low failure stress and strain of the phenol resin [9]. From the stress-strain curves given in Figure 4b the Young's moduli and failure stresses and strains as well as the yield stresses and strains in the case of the plain paper can be derived. These data are summarized in Table 1.

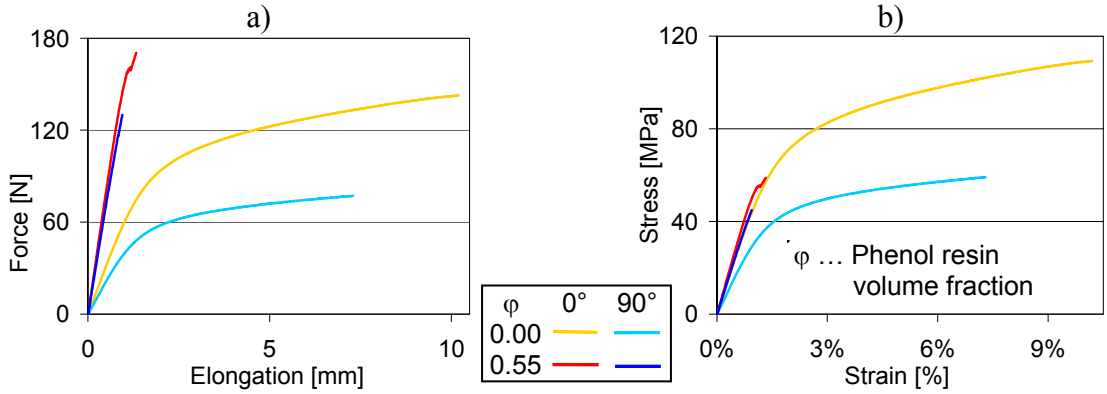

Figure 4: a) Recorded load-elongation functions of different papers and directions,
b) Stress-strain function of the investigated papers

Another important material parameter is the Poisson's ratio. It is defined by the negative ratio of the strain in the loading to the strain in the transverse direction:

$$\nu_{0°/90°} = \frac{-\varepsilon_{90°}}{\varepsilon_{0°}} \,. \qquad (1)$$

In order to determine the Poisson`s ratio experimentally both strains have to be measured simultaneously during testing. Therefore, a second series of tension tests was carried out. This time a universal test machine *H&P Inspect Desk 10* equipped with a 500N load cell was used. The specimens were clamped in special fixtures which were attached parallel and aligned to the crosshead. This was to ensure that the load acts in the centreline of the clamped specimen. The specimens were pulled with 6 mm/min as at the first test series. Both strains in loading and transverse direction were simultaneously measured by a video extensometer during the tests. Black and white labels applied on the specimen marked the measuring points for the extensometer in the loading direction while the specimen edges could be used in transverse direction (Figure 5b).

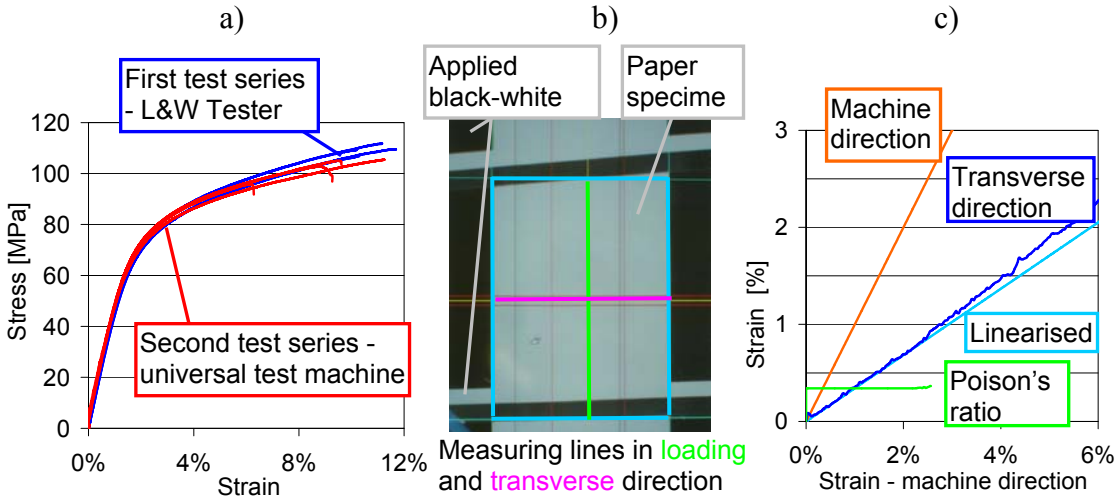

Figure 5: a) Stress-strain function of the two test series,
b) Measurement field of the video extensometer,
c) Measured strains and calculated Poison's ratio

The obtained stress-strain functions agree well with the results of the first test series (Figure 5a). The measured transverse strain curve was approximated by a linear function for the calculation of Poison's ratio (Figure 5c).

Table 1: Mechanical properties of the investigated papers (tension)

Paper	non-impregnated (φ = 0.00)		impregnated (φ = 0.55)	
Specimen direction	0°	90°	0°	90°
Young's Modulus [GPa]	4.97	3.28	5.60	5.02
Failure stress [MPa]	109.3	59.0	54.8	44.5
Failure strain [ ]	0.101	0.073	0.012	0.009
Yield stress [MPa]	60.2	36.8	-	-
Yield strain [ ]	0.014	0.013	-	-
Poison's ratio [ ]	0.340	0.229	0.320	0.293

2.1 Compression test

Particularly, impact events on sandwich structures cause high compressive loading of the sandwich core. In the case of honeycombs this results in a buckling of the cell walls followed by compression failure. Hence, the compressive stiffness and strength of the impregnated paper of the honeycomb cell walls are crucial for the core behaviour and have to be determined.

The standards for paper and board define two test methods to investigate compressive behavior of paper. The short span test of ISO 9895 uses flat fixtures to clamp the specimens. Since the papers used for honeycombs are very thin, this kind of test leads to stability failures at very low load levels. The second method is the ring crush test of ISO 12192, which was chosen in a first approach to determine the required compressive properties. This test method was slightly modified to prevent premature buckling of the specimens and to provide well defined clamping conditions. Figure 6a shows the typical test set-up: the specimen is clamped with clips on the upper and lower support cylinder. Both cylinders as well as a 1kN load cell are attached to a special loading jig. This jig is mounted in a universal test machine *H&P Inspect Desk 50*. In this research all tests were carried out at a constant rate of 0.5 mm/min. The free length between the fixtures was reduced stepwise beginning from 1.0 down to 0.2 mm, leading to an increase of the obtained failure stresses. This result showed that the failure of the tested specimens was caused by buckling, even though the specimens were clamped.

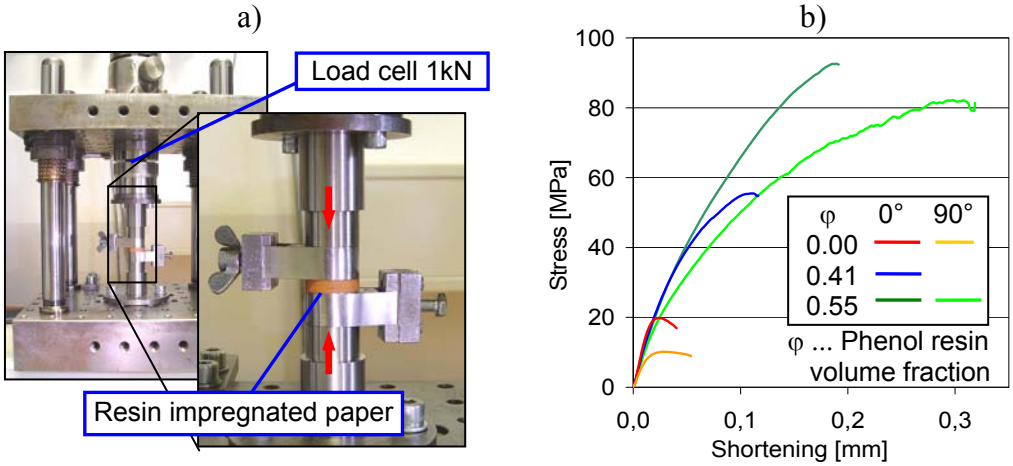

Figure 6: a) Compression test fixture, b) Example of the obtained compressive material characteristics for plain and impregnated paper

The results (Figure 6b) clearly show the influence of different resin volume fractions on the failure stress. The determination of a reliable compressive Young's modulus from the obtained results is not possible.

In a second step the test setup was heavily modified in order to get better test results. The support cylinders were replaced by hardened circular steel plates (Figure 7a), whereas the test machine, the load cell of 1 kN and the loading rate of 0.5 mm/min were maintained. A 15 mm wide and 300 mm long specimen was wound around an aluminium cylinder of 10 mm diameter (Figure 7b). The free edge of the specimen was then fixed using a small adhesive tape. The cylinder was not removed in order to stabilize the specimen and to prevent global buckling during the loading.

With this modified method a second series of tests was carried out. The obtained stress-strain curves are given in Figure 8a. They show after an initial phase a linear behaviour, which permits to determine the Young's moduli. The plain paper specimens failed close to the ends in the 1 mm wide unsupported zones, while the resin impregnated papers rather crushed in the specimen centre.

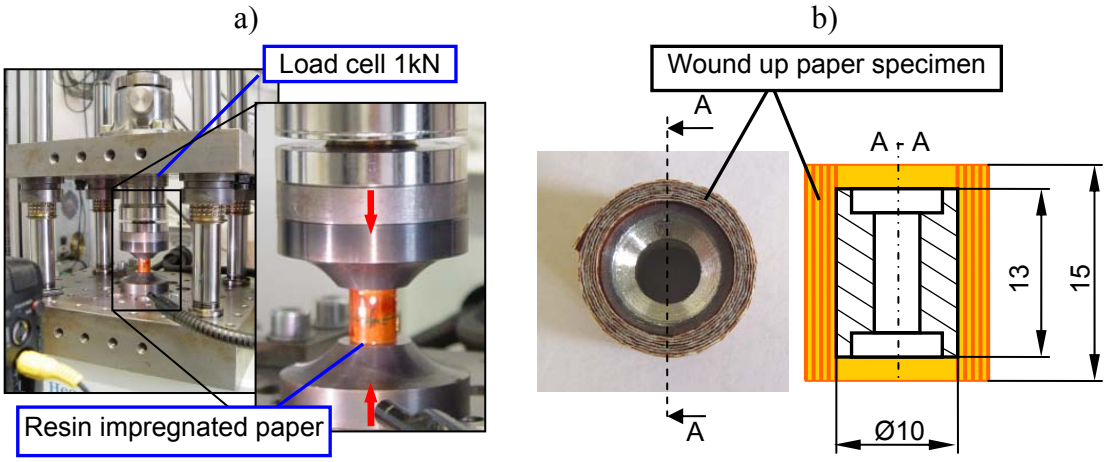

Figure 7: a) Modified compression test setup, b) Prepared paper specimen

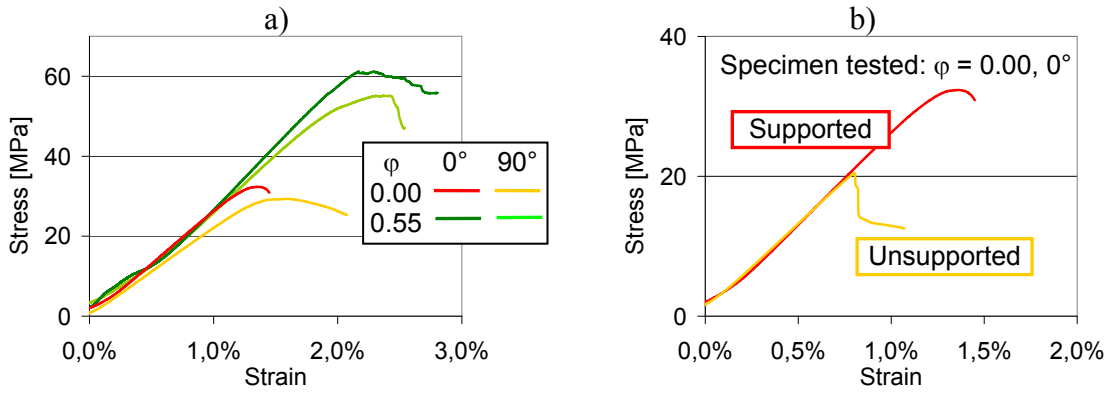

Figure 8: a) Stress strain results of test utilizing the modified compression test setup, b) Material characteristics for supported and unsupported specimens

A further test series was conducted in order to investigate the influence of the aluminium cylinder that supported the specimens. For this purpose the cylinder was removed during testing. An example for the obtained results is shown in Figure 8b, where the stress-strain curves of a supported and a non-supported specimen are compared. It can be clearly seen that the omission of the cylinder leads to a premature

failure caused by global buckling. Below the buckling load the supporting cylinder has no influence on the stress-strain behaviour.

In Table 2 the compressive stiffness of plain and phenol resin impregnated papers are summarized which were determined in this investigation.

Table 2: Obtained compressive stiffness

Paper	Direction	Young's Modulus [GPa]
non-impregnated ($\varphi = 0.00$)	0°	2.66
	90°	2.20
impregnated ($\varphi = 0.55$)	0°	3.20
	90°	3.10

5. NUMERICAL SIMULATION

Various information is gained by experimental investigations of the damage tolerance behaviour of CFRP-sandwich. For example, type and extend of structural damages resulting from impact loading can be obtained by destructive or non-destructive inspection methods. However, fundamental failure mechanisms often are not easily detectable. In these cases finite element simulations offer the opportunity to analyse the failure processes in more detail, including initiation and propagation as well as the prediction of residual strength of damaged structures. Therefore, in this research a numerical analysis of the impact damage process of CFRP-sandwich with honeycomb core was conducted, using the explicit finite element code LS-DYNA. The analysis was based on a meso-mechanical approach [3-6], where the honeycomb cell walls are modelled in detail by 4-node shell elements.

5.1 Validation of the material model for the paper honeycomb core

Before the overall sandwich structure can be analysed an appropriate model has to be provided and validated which represents the mechanical behaviour of the honeycomb cell walls. Thus, simulation models for the tension and compression tests at different papers were developed. Bilinear shell elements and the composite material model MAT58 of LS-DYNA were chosen to describe the orthotropic behaviour of the paper. This constitutive law is an orthotropic so-called elastic damage model, which assumes that deformation causes micro cracks into the material [10, 11]. This approach enables the description of the obtained orthotropic nonlinear stress strain behaviour of the investigated papers. The failure of the material is based on criteria suggested by Hashin [10].

For the simulation of the tension tests a 15 mm wide and 100 mm long piece of paper was modelled. One of the 15 mm wide edges was clamped while on the other one the tension load was applied. The simulation of the plain papers was aborted at a strain of 2.5 %, because the resin impregnated papers failed below that level. This is due to the low failure strain of the phenol resin. As can be seen from the example given in Figure 9 for both plain and resin impregnated papers the simulation results are in good agreement with the experiments. The failure of the plain paper is more ductile, similar to the yielding process known from metallic materials, while the resin impregnated paper fails by brittle fracture.

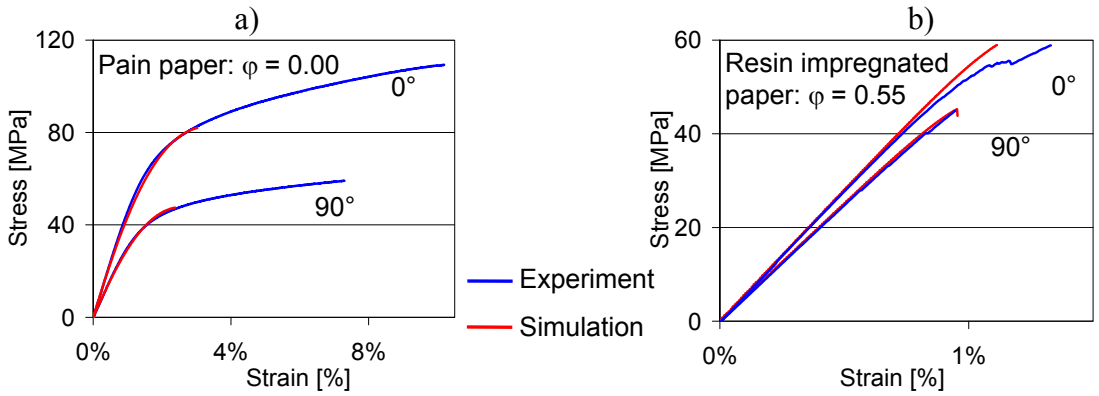

Figure 9: Validation of simulation models for tensile loading: a) plain paper, b) phenol resin impregnated paper

The validation of the compressive behaviour of the investigated papers is based on the compression tests with the coiled paper specimens. The 300 mm long and 15 mm wide specimens were modelled using 4-node shell elements as illustrated in Figure 10a. The aluminium cylinder providing the anti-buckling support as well as the load introduction was modelled by appropriate boundary conditions. Figures 10b and 11 show the simulation results which are in good agreement with the experiments. The supported specimens failed directly at the load introduction or within the 1 mm high unsupported section due to local buckling. Global buckling was the main failure in the case of the unsupported specimens. The validation procedure confirms that a realistic idealisation for both load introduction and buckling support is essential to get reliable simulation results.

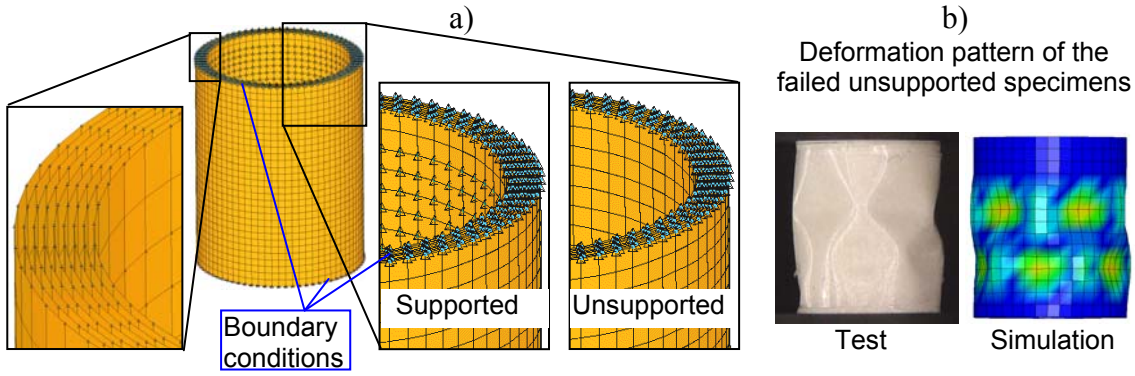

Figure 10: Simulation of the compressive loading: a) finite element model of the coiled paper specimen, b) failure of unsupported specimen

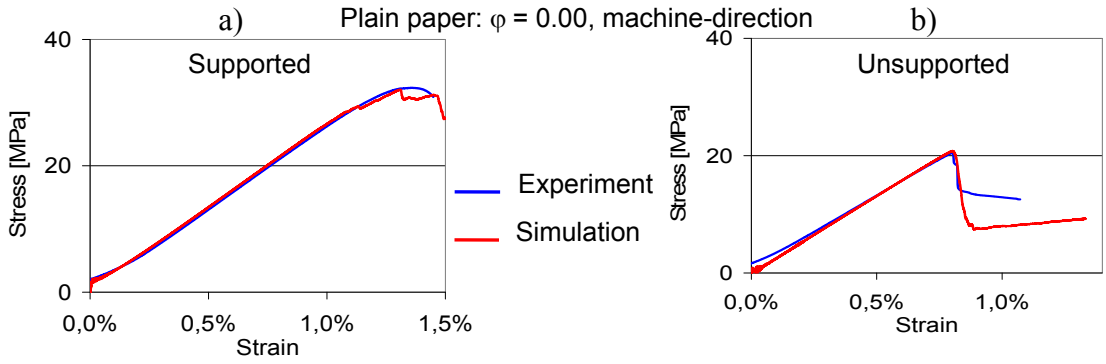

Figure 11: Validation of simulation models for compressive loading: a) supported specimen, b) unsupported specimen

5.2 Impact Simulation

The impact simulations are evaluated using experimental results given in [12]. These impact tests were carried out at different energy levels on honeycomb sandwich specimens which were placed with the back side on a flat support plate. The impactor used had a hemispherical tup of 25.4 mm in diameter.

The top face sheet of the sandwich is composed of five layers of fibre reinforced plastics [(0), (0), (0), (0), (0)]. For the first and the fifth layer 0.1 mm thick glassfibre fabrics are used while the three layers in between consist of 0.211 mm thick carbon fibre fabrics. The back face consists of twenty 0.125 mm thick layers made of unidirectional carbon fibre prepregs and one 0.211 mm thick layer made of carbon fibre fabric with a [0, 0, -45, 45, 90, 90, 45, -45, 0, 0, 0, 0, -45, 45, 90, 90, 45, -45, 0, 0, (0)] stacking sequence. As core material NOMEX®-honeycomb with 4.8 mm wide hexagonal cells and a density of 48 kg/m^3 was used.

Figure 11 shows the finite element model of the sandwich specimen. Both the face sheets and the cell walls of the core are modelled by four-node shell elements. As mentioned before the composite material model MAT58 of LS-DYNA was applied. All necessary material parameters have been obtained from previously measured data.

The bond lines between the face sheets and the cell walls are modelled through cinematic constraints. The base plate as well as the tup are assumed as rigid bodies. This assumption is reasonably, because the stiffness of steel is much higher than the transverse stiffness of the sandwich. Furthermore, the drop weight with the hemispherical tub was modelled by a sphere with a mass of 1.1 kg (Figure 12).

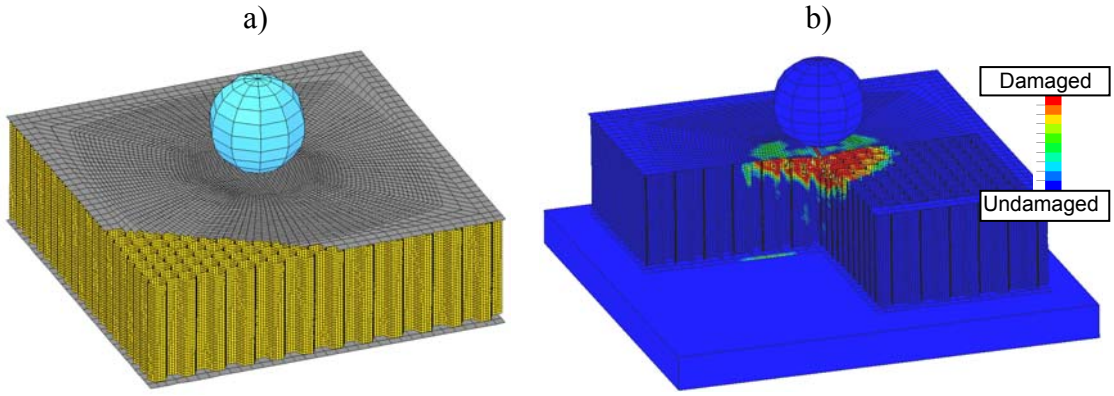

Figure 12: a) Impact simulation model, b) Cross-sectional view of damaged sandwich structure (here: 8J Impact)

Impact simulations were conducted for different energy levels by adjusting the initial speed of the impactor. As an example the results of the 8 Joule impact are given in Figure 13. The calculated force and energy histories shown in Figure 13a agree very well with the experiments. A similar result has been obtained for the local core damage which is depicted in Figure 13b. The core damage marked by red colour in the cross section of the simulation model corresponds quite well with the damaged area found in the test specimen.

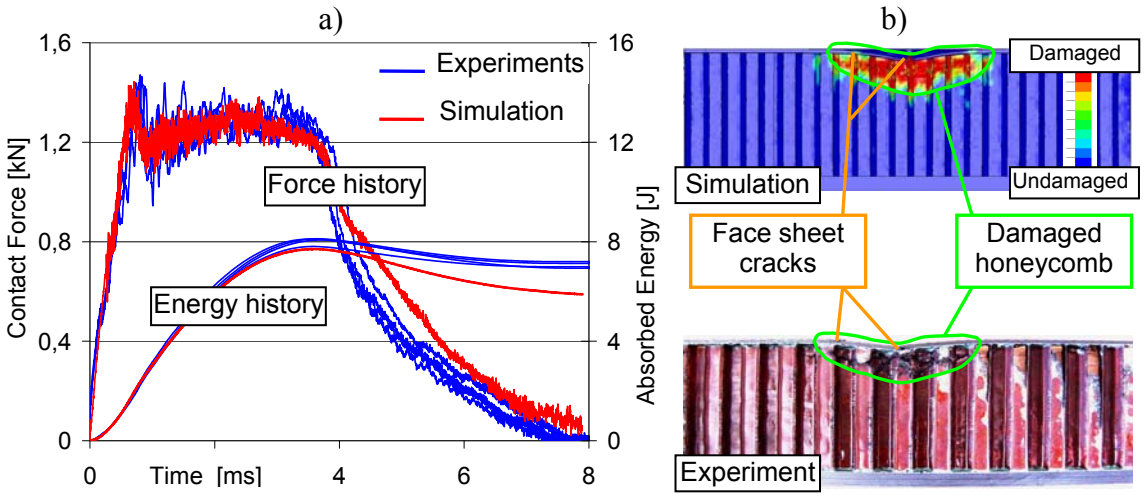

Figure 13: a) Force and energy plots of experiments and simulation (here 8J impact), b) Cross-sectional view of damaged sandwich

6. CONCLUSIONS

A meso-mechanical approach for the numerical simulation of the impact induced damage initiation and propagation in CFRP-sandwich with honeycomb cores is presented. This approach is based on a detailed model of the core structure which requires the mechanical properties of the honeycomb cell walls. These data were determined using a standard tension and a newly developed compression test. Papers with different phenol resin volume fractions were examined. One of the findings was that the investigated papers show a distinct orthotropic behaviour. Another basic result was that the stress-strain relation strongly depends on the resin fraction. The plain paper has a ductile behaviour, whereas paper with a high resin fraction is rather brittle.

The tests performed on various papers were simulated to validate the material model that is used to describe the honeycomb cell wall properties. This model is the basis for the numerical simulation of the damage tolerance behaviour of sandwich structures.

Finally, based on the described approach simulations of impacts on CFRP-sandwich plates with NOMEX®-honeycomb cores were conducted. The computed structural response as well as the predicted face sheet and core damages are in good agreement with the experiments. The results of the presented investigation clearly show that experimentally determined properties of the cell wall materials are essential for a reliable prediction of the damage tolerance behaviour of honeycomb sandwich.

ACKNOWLEDGEMENTS

The plain and resin impregnated papers were provided by Mr. M. Seidel from SCHÜTZ GmbH & Co. KGaA. His support is gratefully acknowledged.

REFERENCES

1- Besant, T., Davies, G. A. O. and Hitchings, D., "Finite element modelling of low velocity impact of composite sandwich panels", *Composites Part A: Applied Science and Manufacturing*, 2001;32:1189-1196.

2- Meo, M., Vignjevic, R. and Marengo, G., "The response of honeycomb sandwich panels under low-velocity impact loading", *Intern. Journal of Mechanical Sciences*, 2005;47:1301-1325.

3- Battilomo, L., Marchetti, M. and Severoni, R., "Global residual damage evaluation of impacted sandwich panels at low energy", *ICAS 2000 CONGRESS,* 2000;-:434.1-434.9.

4- Hähnel, F. and Wolf, K., "Numerical simulation of CFRP honeycomb sandwich subjected to low-velocity impact", *Proceedings of Conference on Sandwich Construction 5*, Zürich, 2000;2:657-666.

5- Hähnel, F. and Wolf, K., "Evaluation of the material properties of resin-impregnated NOMEX® paper as basis for the simulation of the impact behaviour of honeycomb sandwich", *Proceedings of Conference on Composite Testing and Material Identification*, Porto, Portugal, 2006.

6- Foo, C.C., Chai, G.B. and Seah, L.K., "A model to predict low-velocity impact response and damage in sandwich composites", *Composite Science and Technology,* 2008;68:1348-1356.

7- Foo, C. C., Chai, G. B. and Seah, L. K., "Mechanical Properties of Nomex Material and Nomex Honeycomb Structure", *Composite Structures*, 2007;80:588-594.

8- n.n., "Schütz Coremaster – The lightweight structure fore highest requirements", Schütz Industry Service, *http://schuetz.de/schuetz/de/industry_services/service/downloads/cormaster_brosch_gb.pdf.*

9- Åström. T., "Manufacturing of Polymer Composites", *Chapman & Hall*, 1997.

10- Matzenmiller, A., Lubliner, J. and Taylor, R.L., "A constitutive model for anisotropic damage in fiber-composites", *Mechanics of Material*, 1995;20:125-152.

11- Schweizerhoff, K., Weimar, K., Münz, Th. And Rottner, Th., "Crashworthiness analysis with enhanced composite material models in LS-DYNA merits and limits", *Proceedings of 5th international LS-DYNA User Conference*, Detroit, Michigan, USA, 1998.

12- Kolax, M., "Multifunctional integral structures of fibre reinforced composites (EMIR) - engineering of an advanced fuselage of the next generation", *Lufo3 cooperative project CORUBA*, Project no. 20W0301A, 2003-2007